J Fluoresc (2014) 24:1003–1014
DOI 10.1007/s10895-014-1361-8

ORIGINAL PAPER

Excimer Emission in Norepinephrine and Epinephrine Drugs with α- and β-Cyclodextrins: Spectral and Molecular Modeling Studies

N. Rajendiran · T. Mohandoss · J. Thulasidasan

Received: 24 October 2013 / Accepted: 3 February 2014 / Published online: 31 May 2014

Abstract The inclusion complexation behavior of norepinephrine (NORE) and epinephrine (EPIN) with native cyclodextrins (α-CD and β-CD) were investigated by UV-visible, fluorimetry, time-resolved fluorescence, SEM, TEM, FT-IR, ^{1}H NMR, DSC, powder XRD and PM3 methods. Single emission was observed in aqueous solution where as dual emission (excimer) noticed in the CD solutions. Both drugs form 1:1 drug-CD complexes in lower CD concentrations and 1:2 CD-drug$_2$ complexes in the higher CD concentrations. Time-resolved fluorescence studies indicated that both drugs showed single exponential decay in water and biexponential decay in CD. Nano-sized self-aggregated particles of drug-CD were found by TEM studies. Molecular modeling studies indicated that aliphatic chain part of the drug was entrapped in the CD cavity. Thermodynamic parameters and binding affinity of complex formation of the CD were determined according to PM3 method. The PM3 results were in good agreement with the experimental results.

Keywords Cyclodextrin · Norepinephrine · Epinephrine · Excimer · Nanoparticles · Molecular modeling

Introduction

Norepinephrine or noradrenaline [1-(3,4-dihydroxyphenyl)-2-aminoethanol, NORE] is a catecholamine used to elevate blood pressure, in the case of shock or haemorrhage, and as a peripheral vasoconstrictor. Catecholamines are hormones released by adrenal glands and neurotransmitters of the sympathetic and central nervous system. Such substances are biosynthesized from tyrosine. Catecholamines control the nervous system in a series of biological reactions and chemical processes [1, 2]. Epinephrine or adrenaline [1-(3,4-dihydroxyphenyl)-2-methyloaminoethanol, EPIN] also belongs to the catecholamine family and plays an important role as neurotransmitters and hormones. It is biosynthesized in the adrenal medulla and sympathetic nerve terminals, as well as being secreted by the suprarenal gland along with norepinephrine. It is used in medicine in the treatment of heart attack, bronchial asthma and cardiac surgery [3, 4]. Because of its poor aqueous solubility, the therapeutic use of both drugs is limited to topical applications.

In the recent years, to resolve bioavailability problems related to poor solubility and the low dissolution rate of drugs in biological fluids, different approaches have been investigated. As widely reported in literature, cyclodextrins (CDs) are regarded as most functional and enabling excipients which via dynamic complex formation interact with many water insoluble drugs or their lipophilic moieties thereby increasing undesirable physicochemical properties including low aqueous solubility, poor dissolution rate, and limited drug stability [5, 6]. Cyclodextrins are cyclic oligosaccharides derived from starch containing six (α-CD), seven (β-CD), eight (γ-CD) or more (α-1,4)-linked α-D-glucopyranose units [7]. They are cylinder-shaped and possess a cage-like supramolecular structure [8]. The polarity of the cavity has been estimated to be similar to that of an aqueous ethanolic solution [9]. Cyclodextrins exhibit a hydrophilic exterior and a hydrophobic internal cavity in which lipophilic soluble drugs may form inclusion complexes.

The aim of this study was to investigate the formation of inclusion complex between NORE or EPIN and CD (α-CD/β-CD). Drug-CD interactions in solution were investigated by absorption, fluorescence and time-resolved fluorescence measurements. The solid state inclusion complexes was performed

Electronic supplementary material The online version of this article (doi:10.1007/s10895-014-1361-8) contains supplementary material, which is available to authorized users.

N. Rajendiran (✉) · T. Mohandoss · J. Thulasidasan
Department of Chemistry, Annamalai University,
Annamalai nagar 608 002, Tamil Nadu, India
e-mail: drrajendiran@rediffmail.com

by scanning electron microscopy (SEM), transmission electron microscopy (TEM), Fourier transform infrared spectroscopy (FT-IR), proton nuclear magnetic resonance (^{1}H NMR), differential scanning calorimetry (DSC) and powder X-ray diffractometry (XRD).

Material and Methods

Materials

Norepinephrine (NORE), epinephrine (EPIN), α-CD and β-CD were purchased from Sigma -Aldrich chemical company and used as such.

Preparation of Inclusion Complexes in Solutions

Triply distilled water was used for the preparation of all aqueous solution. A serious of samples with constant concentration of fluorophores (NORE and EPIN drugs) and different concentration of α-CD and β-CD were prepared. The concentration of the drug solutions were maintained at 4×10^{-5} M and the CD concentration were varied from 1×10^{-3} to 1×10^{-2} M. The mixture of drug-CD solution were shaken thoroughly and kept for 6 h to bring it to a state of equilibrium. The experiments were carried out at room temperature 303 K. The solid inclusion complexes are prepared by coprecipitation method. The obtained powder samples were analysed by SEM, TEM, FT-IR, DSC, ^{1}H NMR and powder XRD methods.

Instruments

Absorption and fluorescence spectral measurements were carried out with Shimadzu UV-visible spectrophotometer (model 1601 PC) and Shimadzu spectrofluorimeter (model RF-5301), respectively. The SEM photographs were collected on a Hitachi S3400N. The morphologies of nano-encapsulated complexes NORE/CD and EPIN/CD were investigated by TEM using TECNAI G^4 microscope with accelerating voltage 200 kV. FT-IR spectra of powder sample of drug, α-CD, β-CD and the inclusion complexes were measured from 4,000 cm^{-1} to 400 cm^{-1} on JASCO FT-IR-5300 spectrometer using KBr pellet. Thermal characteristics of solid inclusion complexes were measured using Mettler Toledo DSC1 fitted with STRe software (Mettler Toledo, Switzerland). The temperature scanning range was from 25 to 230 °C with a heating rate of 10 °C/min. One-dimensional ^{1}H NMR spectra for the drugs and the inclusion complexes were recorded on a Bruker AVANCE 500 MHz spectrometer (Germany). Samples were dissolved in DMSO-d6 (99.98 %) and were equilibrated for at least 1 h. XRD patterns of powder samples were recorded with a BRUKER D8 Advance diffractometer (Bruker AXS GmbH, Karlsruhe, Germany) with Cu KαI radiation (λ=1.5406 Å), a voltage of 40 kV and a 20 mA current.

The fluorescence lifetime measurements were performed using a picoseconds laser and single photon counting setup from Jobin-Vyon IBH. A diode pumped Millena CW laser (Spectra Analysis) 532 nm was used to pump the Ti-Sapphire rod in Tsunami picosecond mode locked laser system (Spectra physics Model No. 4690 M3S). The Ti-Sapphire rod is oriented at Brewster's angle to the laser beam. The wavelength turning range was 280–540 nm, i.e., standard pico configuration. The fluorescence decay of the sample was analysed using IBH data analysis software. The fluorescence decay profiles were fitted to the expression:

$$I(t) = A_1\exp\left(\frac{-t}{\tau_1}\right) + \mathrm{A}_2\ \exp\left(\frac{-t}{\tau_2}\right) \tag{1}$$

$$I(t) = A_1\exp\left(\frac{-t}{\tau_1}\right) + \mathrm{A}_2\exp\left(\frac{-t}{\tau_2}\right) + \mathrm{A}_3\exp\left(\frac{-t}{\tau_3}\right) \tag{2}$$

Where τ_1, τ_2 and τ_3 are lifetimes of the three components, a_1 a_2 and a_3 are the pre-exponential factors of the same and t is time. The average fluorescence lifetime was calculated using the equation:

$$\langle\tau\rangle = \sum \tau_i a_i \tag{3}$$

Molecular Modeling

The theoretical calculations were performed with Gaussian 03 W package. The initial geometry of the drugs, α-CD and β-CD were constructed with Spartan 08 and then optimized by PM3 (Parametric method 3). CD was fully optimized by PM3 without any symmetry constraint [10, 11]. The glycosidic oxygen atoms of CD were placed onto the XY plane and their center was defined as the center of the coordination system. The primary hydroxyl groups were placed pointing toward the positive Z axis. The inclusion complexes were constructed from the PM3-optimized CD and guest molecules. The longer dimension of the guest molecule was initially placed onto the Z axis. The position of the guest was determined by the Z coordinate of one selected atom of the guest. The inclusion process was simulated by putting the guest in one end of CD and then letting it pass through the CD cavity.

Results and Discussion

Effect of Cyclodextrins on NORE and EPIN

Table 1 and Figs. 1 and 2 depict the absorption and fluorescence maxima of NORE and EPIN drugs in pH ~7 solutions

containing various concentrations of α-CD and β-CD. The insets in Figs. 1 and 2 depict the changes in the absorbance and fluorescence intensity observed as a function of different concentrations of CD. The absorption spectra of both drug molecules consist of two peaks at ~275 nm and ~225 nm. Upon increasing the CD concentrations, absorbance of both drugs increased and the maximum was slightly red shifted. The above results indicated that both drug molecules are transferred from more protic environments (bulk aqueous phases) to less protic CD nano-cavity environments [12–16]. Absorption and fluorescence spectral shifts and shapes of EPIN:CD inclusion complexes are similar to NORE:CD inclusion complexes suggesting that both drugs form similar type of inclusion complexes.

Figure 2 shows the emission spectra of NORE and EPIN drugs (excited at 280 nm) with varying concentrations of α-CD and β-CD. In aqueous medium, both drugs show single emission at ~316 nm whereas dual emission obtained in CD medium (Table 1). In both CD solutions, a new longer wavelength (LW, ~450 nm) emission was observed. With an addition of drugs into the CD solutions, the SW emission intensities were decreased at the same wavelength. However in CD solutions, the LW intensity is regularly increased. Even in very low CD concentration (at 1×10^{-3} M) LW emission can be detected in the above drugs. This LW emission attributed to the formation of drug-CD inclusion complex. The fluorescence spectral results indicated that the drugs were encapsulated in the hydrophobic CD nano-cavities [12–16]. At higher CD concentrations, the similar absorption and emission maxima for the drugs indicating the formation of the similar inclusion complexes.

Excimer Emission

The LW emission in the CD solution can be explained as follows: With an increase in the CD concentration, emission intensity of the LW band was increased significantly, whereas the SW band was decreased. The LW emission in NORE and EPIN drugs presumably ascribed at least two types of inclusion complexes exist in the aqueous CD solution. The strong SW emission around 316 nm was due to the monomer inclusion complex (1:1) and the weak LW emission was attributed to the excimer fluorescence of NORE and EPIN drugs. In higher CD concentration (1×10^{-2} M), the amount of excimer inclusion complexes were increased; therefore that only the excimer band intensity increased while the monomer band intensity decreased. These opposite spectral changes in SW and LW band suggest that the structural geometry of the inclusion complexes is different in terms of the orientations of the guest molecule. The drug excimer fluorescence (LW) was due to a formation of 1:2 CD-drug inclusion complex formed by the self-association of the drugs within the CD cavity [14, 17].

When the dilute drug (2×10^{-6} M) solution containing CD was excited, no excimer fluorescence was observed (Figure not shown). This indicates that the formation of 1:1 CD-drug inclusion complexes, the self-association, or in other words, the excimer occurred at a higher concentration of the drugs. These findings suggest that 1:1 CD-drug inclusion complexes alone exist in the dilute solution of the drugs.

$$\text{CD} + \text{drug} \overset{K_1}{\rightleftarrows} \text{CD-drug} \tag{4}$$

Here drug stands for NORE and EPIN, K_1 is the equilibrium constant for the 1:1 inclusion complex. Benesi-Hildebrand equation was used for determining the binding constant (K_1) from the absorption and fluorescence intensity change by the addition CDs.

$$\frac{1}{\left(I_f - I_f{}^0\right)} = \frac{1}{a} + \frac{1}{\left(aK_1[CD]_0\right)} \tag{5}$$

where 'I_f' and '$I_f{}^0$' are the fluorescence intensity in the presence and absence of CD respectively, 'a' is the constant and $[CD]_0$ is the initial concentration of the CD solution [17, 18]. The double reciprocal plot shown in Figs. 3 and 4 give upward or downward curves for the NORE/CD and EPIN/CD complexes indicating that the inclusion complexes are not 1:1 stoichiometry.

Now considering the excimer in the CD-drug system, there are two possibilities for excimer formation scheme. One possibility is that excimer emitting species may be 2:2 CD-drug inclusion complex [$(\text{CD-drug})_2$] and the other possibility is a 1:2 [CD-drug_2] inclusion complex. But in the NORE and EPIN drugs, 1:2 inclusion complex was responsible for the excimer fluorescence. This type of inclusion complex was formed through the following equilibrium

$$\text{CD-drug} + \text{drug} \overset{K_2}{\rightleftarrows} \text{CD-}(\text{drug})_2 \tag{6}$$

where K_2 is the equilibrium constant for the formation of the 1:2 inclusion complex. When the above described scheme is true, the excimer fluorescence intensity should be proportional to the concentration of the 1:2 CD-drug inclusion complexes. Thus, comparisons were made between the CD concentration dependence of the observed excimer fluorescence intensity and simulation curves for the CD-$(\text{drug})_2$ concentration, which was calculated using the estimated K_2 as shown in the following equations:

$$\left[CD{-}(drug)_2\right] = \left([drug]_0 - [drug] - [CD{-}drug]\right)/2 \tag{7}$$

$$2K_1K_2[CD]_0^2[drug]^2 + \left(1 + K_1[CD]_0\right)[drug] - [drug]_0 = 0 \tag{8}$$

Here, $[\text{drug}]_0$ and [drug] are the initial concentration of drug and the concentration of free drug, respectively.

Table 1 Absorption and fluorescence maxima (nm) of NORE and EPIN at different concentrations of α-CD and β-CD

Concentration of CD M	NORE						EPIN					
	α-CD			β-CD			α-CD			β-CD		
	λ_{abs}	log ε	λ_{flu}	λ_{abs}	log ε	λ_{flu}	λ_{abs}	log ε	λ_{flu}	λ_{abs}	log ε	λ_{flu}
Water (without CD)	275	3.334	316	275	3.334	316	275	3.30	318	275	3.30	318
	225	0.38		225	0.38		226	4.39		226	4.39	
0.002	279	3.494	316	279	3.494	316	279	3.504	318	280	3.504	318
	224	0.30	450	224	0.30	450	224	0.33	450	220	0.33	450
0.006	280	3.584	316	279	3.584	316	280	3.56	318	280	3.56	318
	223	0.36	450	223	0.36	450	224	4.37	450	220	4.37	450
0.010	280	3.754	316	280	3.754	316	280	3.73	319	280	3.73	319
	223	0.43	450	225	0.43	450	223	4.42	450	220	4.42	450
Excitation wavelength (nm)			270			270			270			270
K (M^{-1})	124		289	356		579	132		312	375		612
ΔG (kcal.mol^{-1})	−2.90		−3.41	−3.53		−3.82	−2.93		−3.45	−3.56		−3.86

Figure 5 shows the best fit curve of CD-$(drug)_2$ estimated with K_2(CD). The quality of the fit to the observed intensity data was satisfactory which indicates that the LW emission was due to the 1:2 excimer [CD-$(drug)_2$] inclusion complex formation. The proposed 1:2 CD-drug inclusion complex structures are given in Fig. 6.

The free energy change was calculated from the formation constant (K) as follows:

$$\Delta G = -RT\ln K \tag{9}$$

The ΔG values for the formation of the inclusion complexes are given in Table 1. As can be seen from the Table 1,

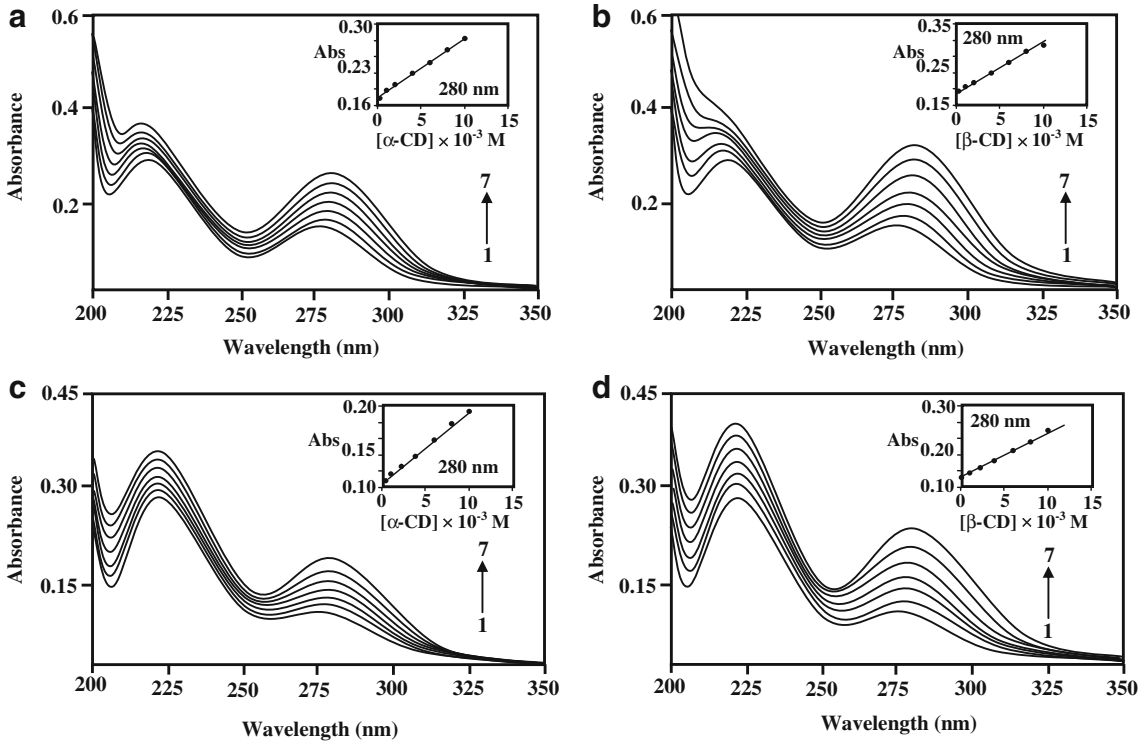

Fig. 1 Absorption spectra of **a**, **b** NORE and **c**, **d** EPIN in different α-CD and β-CD concentrations (M): (*1*) 0, (*2*) 0.001, (*3*) 0.002, (*4*) 0.004, (*5*) 0.006, (*6*) 0.008, (*7*) 0.01. *Insert Fig.*: Plot of absorbance vs. CD concentrations

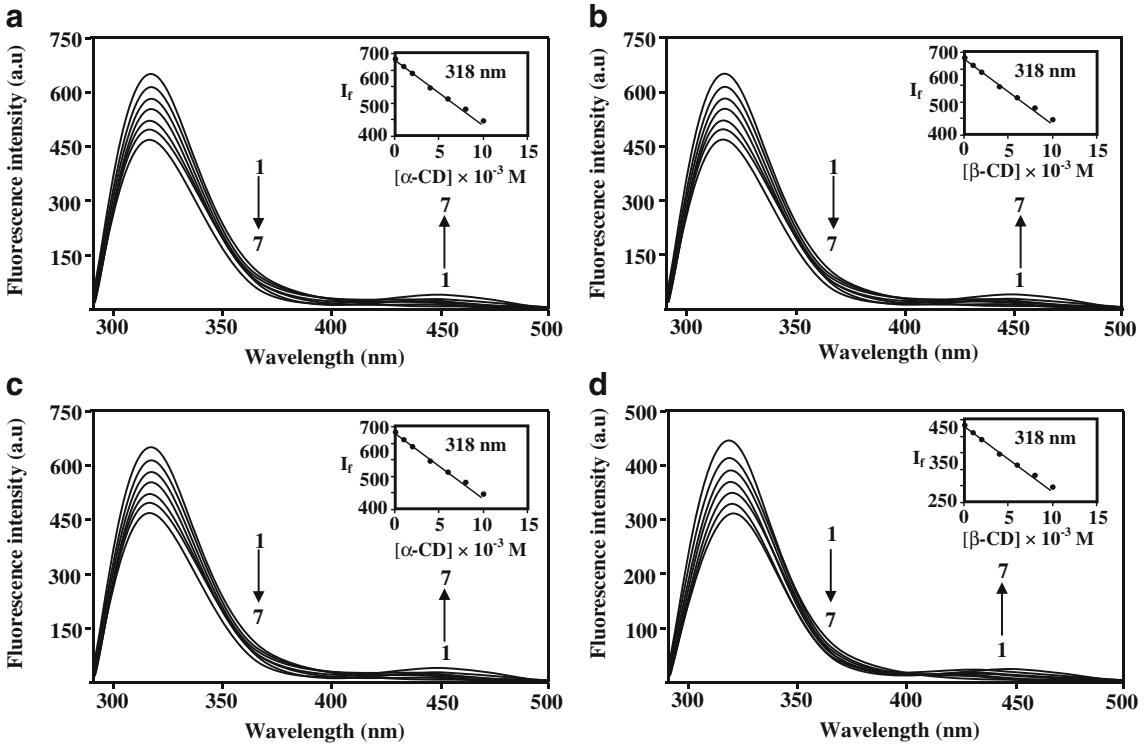

Fig. 2 Fluorescence spectra of **a**, **b** NORE and **c**, **d** EPIN in different α-CD and β-CD concentrations (M): (*1*) 0, (*2*) 0.001, (*3*) 0.002, (*4*) 0.004, (*5*) 0.006, (*6*) 0.008, (*7*) 0.01. *Insert Fig.*: Plot of fluorescence intensity vs. CD concentration

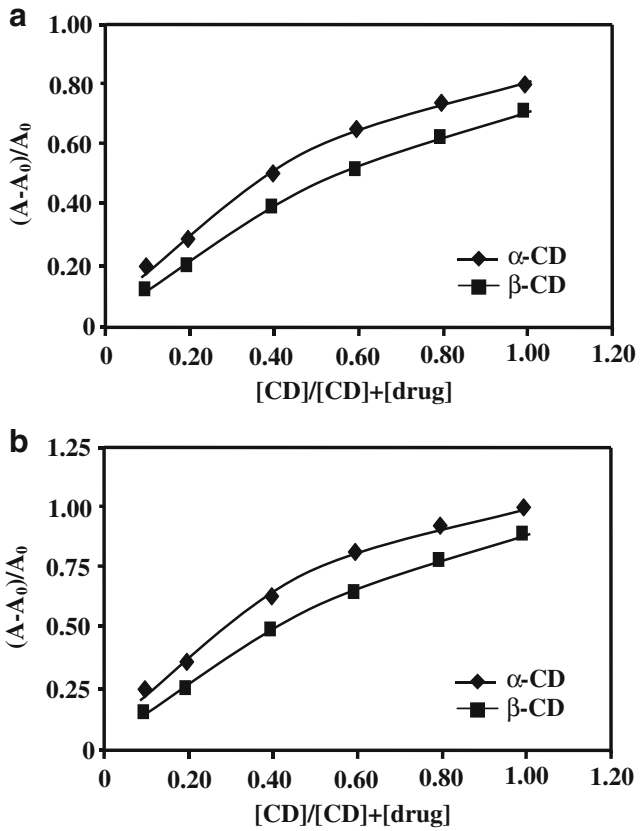

Fig. 3 Double reciprocal plot $(A-A_0)/A_0$ versus [CD]/[CD] + [drug] for 1:1 inclusion complex formation of **a** NORE and **b** EPIN

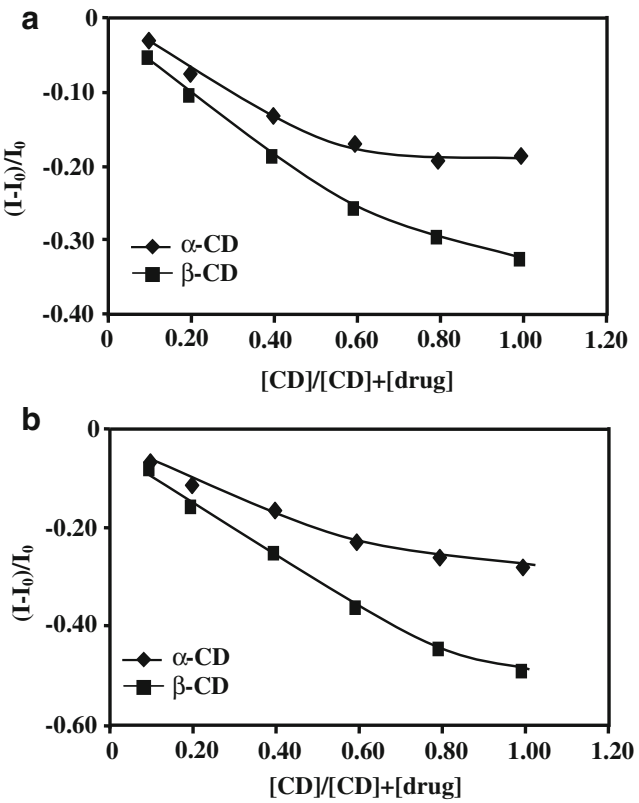

Fig. 4 Double reciprocal plot $(I-I_0)/I_0$ versus [CD]/[CD] + [drug] for 1:1 inclusion complex formation of **a** NORE and **b** EPIN

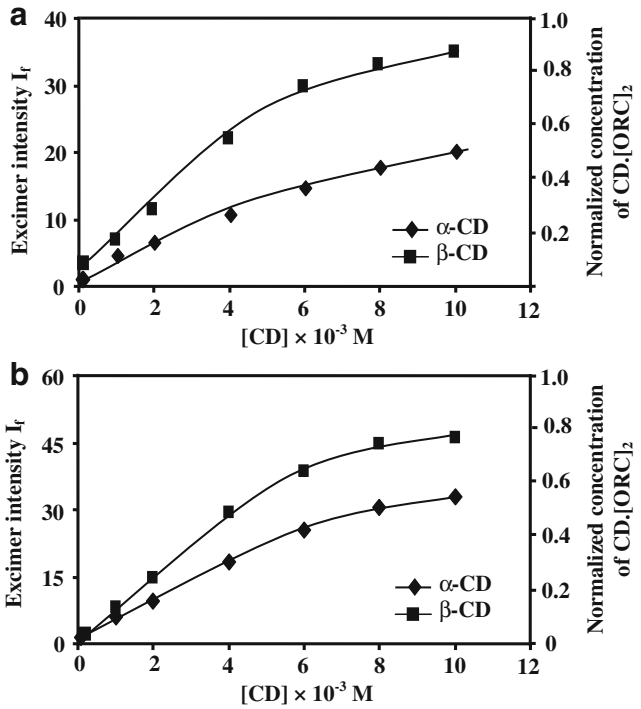

Fig. 5 Comparison between the concentrations curves calculated for the 1:2 CD-drug inclusion complexes and the observed excimer fluorescence intensities of **a** NORE and **b** EPIN with CDs

ΔG is negative which suggests that the inclusion proceeded simultaneously at 303 K. The experimental results are indicating that the inclusion reactions of the CD with the drugs are an exothermic process.

Prototropic Reaction in CD Medium

The effect of CD on the prototropic equilibrium between neutral and monoanion changes in the absorption and emission spectra in both CD solutions were measured. The absorption and emission maxima of drugs in CD solutions were studied in 6×10^{-3} M in the pH range 0.1–11. When increase the pH from ~7 to 10, the SW band at ~317 nm was not changed, whereas the LW band continuously red shifted. The above results suggest that the formation of monoanion (deprotonation of OH group) in any one the hydroxy group present in the drug molecules [14, 19]. The above results may be possible, if the hydroxy group of the drugs presents in the bulk aqueous environment and the alkyl chain resides inside of the CD cavity.

Time-Resolved Fluorescence Measurements

Fluorescence lifetime measurement has long been recognized as a sensitive indicator for monitoring excited state affairs of a fluorophore [20–23]. With a view to achieve a deeper insight into the excited state photophysics of the studied drugs and its alterations under CD confinement, we were recorded the fluorescence lifetimes of the above drugs in different environments. The excitation wavelength was 290 nm and the emission wavelength was 315 nm. The typical time-resolved fluorescence decay profiles demonstrating that the fluorescence decay was significantly affected by the concentration of CD and the results are summarized in Table 2. The fluorescence decay behavior of drugs both in water and in CD environments was found to be quite different.

In both drugs, single-exponential fluorescence decay was observed in water. However, in the presence of CD solution (0.01 M), the fluorescence decays are fitted to bi-exponential indicating the presence of at least two excited state species of drug when complexed to CD with lifetimes of τ_1 and τ_2. The decay values in the CD solutions (NORE: α-CD- τ ~ 0.1.26 ns, β-CD-τ ~ 3.18 ns; EPIN: α-CD-τ ~ 1.70 ns, β-CD- τ ~ 3.41 ns) are significantly higher than those observed in water (NORE: τ ~ 0.29 ns; EPIN: τ ~ 0.43 ns), which illustrate considerable change in the microenvironment of guest upon entrapment into the hydrophobic CD cavities. The tri-exponential analysis was also attempted on the same set of conditions. A consistent enhancement of lifetimes of drugs with the addition of CD (0.01 M) well matches our previous interpretation of the steady-state fluorescence data, indicating the formation of inclusion complex between guest and CD molecules. The enhanced lifetimes associated with CD concentration leads to restriction of rotational degrees of freedom with consequent impact on depletion of non-radiative decay channels. Further compared to α-CD, the efficiency of lifetime increasing is found to be higher with β-CD (Table 2) which shows the stronger hydrophobic interaction between drugs and β-CD.

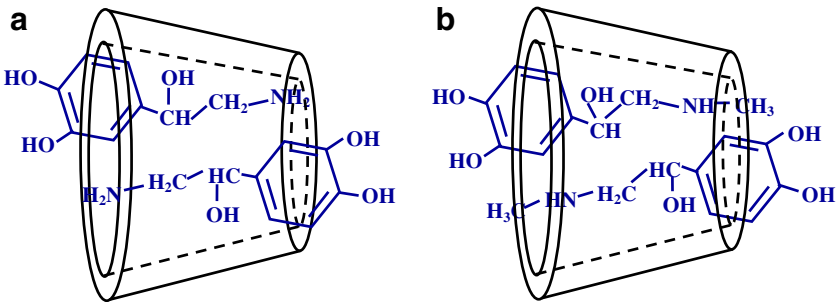

Fig. 6 The proposed 1:2 CD-drug inclusion complex structure of **a** NORE/CD and **b** EPIN/CD

Table 2 Fluorescence decay parameters of EPIN and NORE in water, α-CD (0.01 M) and β-CD (0.01 M) solutions

Drugs	Medium	Lifetime (ns)		Pre exponential factor		<τ>
		τ_1	τ_2	a_1	a_2	
NORE	Water	0.29		0.98		0.29
	α-CD	0.52	1.79	0.70	0.30	1.26
	β-CD	0.95	4.58	0.72	0.28	3.18
EPIN	Water	0.43		0.99		0.43
	α-CD	0.55	2.83	0.80	0.20	1.70
	β-CD	0.34	4.75	0.0.84	0.16	3.41

Molecular Modeling Studies

To further probe the mode of interaction between the drug molecules (NORE, EPIN), α-CD and β-CD, a molecular modeling (semi-empirical quantum mechanics) study was conducted at PM3 method. Complete geometry optimizations without any restriction were employed in the study of the complexation process of the above drug molecules with α-CD and β-CD. The most energetically favourable structures of the drug molecules as well as CD molecules were used to construct CD inclusion complexes. The inclusion complexes were constructed by manually inserting the drug into the CD cavity through the wider rim, centering it on a vector perpendicular to the mean plane through the glycosidic oxygen atoms.

For the simulation process, CD was kept in this position while the drug approached along the z-axis towards the wider rim of CD cavity. The orientations of the drug deduced from the results of the investigations in solution were considered. The relative position between drug and CD was calculated by the distance of C_4 atom of guest and the secondary rim of host molecule. The drug was initially located at a distance of 6 Å from the cavity rim and then moved in decreasing increments of 2 Å towards the center of the CD cavity. At each step the whole inclusion structure was fully optimized without any constraint using the PM3 method in Gaussian 03 package. So the guest molecule was free to move in the CD cavity during the entire optimization process. Therefore, the conformational changes of the drug and CD molecule were explicitly allowed. In this way, the local minima for all the inclusion complex structures were found and further optimized with PM3 level.

Figure 7 displays the upper and side view of the most stable inclusion complexes of NORE and EPIN, respectively. In all the complex structures, a considerable part of the guest molecule is accommodated in the cavity of CD. The long axis of the drug is oriented along the axis of the CD, with the alkyl chain positioning within the cavity. The minimum energy structure also revealed that drugs were included along the molecular axis of CD, but its molecular axis was not exactly perpendicular to the CD symmetry axis, rather it was slightly tilted to allow maximum hydrogen bonding between the host and the guest. In both cases, the preferred orientation for complex formation is that one, in which the benzene ring of guest is located near at the wider rim comprising the secondary hydroxyl groups. More importantly the simulation results are in good agreement with the experimental data. Compared to phenyl ring, the alkyl chain is more deeply associated with the CD cavity, consistent with the significant increase in the LW emission of the drug due to complex formation.

The binding energies (ΔE) for different 1:1 drug-CD inclusion complexes are given in Table 3. The binding energies (ΔE) suggest that isolated drugs are highly miscible with β-CD. Further the change in the magnitude of the ΔE would be a sign of the driving force towards complexation. The more negative ΔE value indicates the complex is more thermodynamically favorable. From the energy point of view, it could be concluded that the binding energies of EPIN/CD complexes were 0.91 kcal mol^{-1} (for α-CD) and 1.56 kcal mol^{-1} (for β-CD) lower than that of NORE/CD complexes. The calculated binding energies for the obtained complexes were in sequence of EPIN/β-CD > NORE/β-CD, EPIN/α-CD > NORE/α-CD. The above sequence revealed that the EPIN drug formed more stable inclusion complexes with β-CD in comparison to the other CD complexes. However, the systems, as in the case of four inclusions, exhibited a better compatibility, as ascertained from their binding energy (Table 3).

Further studies on the geometrical structures of the inclusion complexes were also made, in order to explore the stability of these complexes. In Fig. 7 it can be seen that the drugs are almost encapsulated in the cavity of CD molecules. In addition, there are several intermolecular H-bondings in the structures. Here, the H-bondings are defined as C-H···O or C-H···N with the distance $d_{H\cdots O}$ or $d_{H\cdots N}$ less than 3.0 Å [24]. These findings indicated that intermolecular H-bonds played a crucial role in the stability of the inclusion complexes. Considering the shape and dimensions of the host, the guests may not be completely embedded into the CD cavity. Since the vertical distance and length of the guests were greater than the dimensions of the host, the guest molecules cannot be fully present in the inside of the CD cavity. Further, the optimized theoretical structures of the guest/CD inclusion complex also confirmed that the guest molecules were partially included in the CD cavity.

The PM3 optimized structural parameters, namely the bond distances, bond angles and dihedral angles of the above drug molecules before and after complexation in α-CD and β-CD obtained from the PM3 most stable structures are presented in Table S1. The calculated parameters evidently showed that the geometry of the guest distorted. It was also found that a great distortion in dihedral angles when compared to other

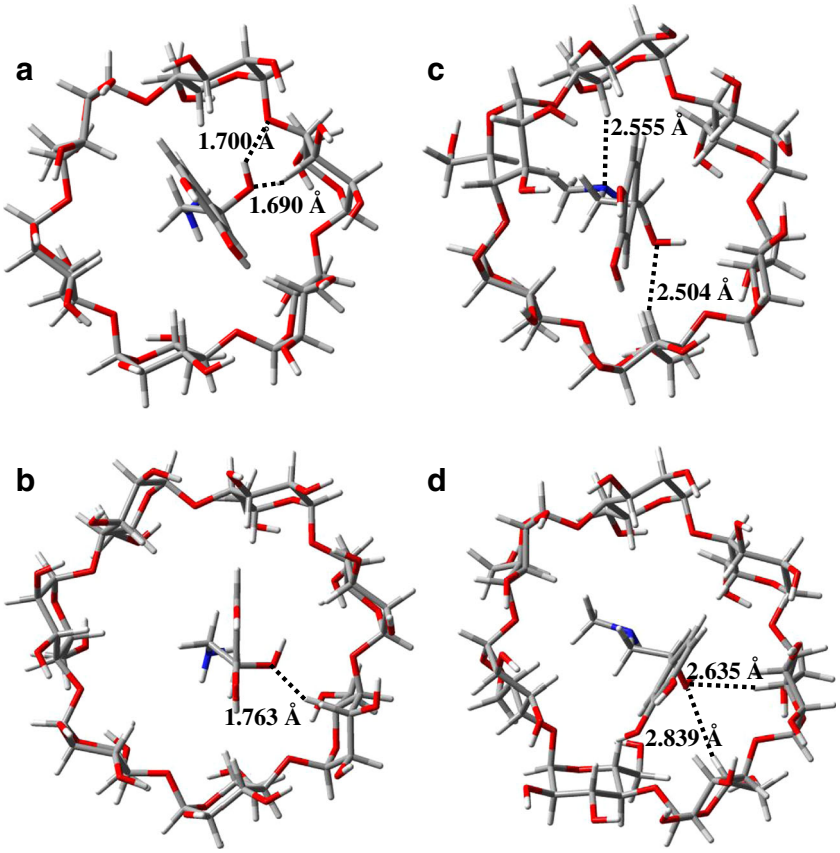

Fig. 7 Upper views of PM3 optimized structures of inclusion complexes **a** NORE/α-CD, **b** NORE/β-CD, **c** EPIN/α-CD and **d** EPIN/β-CD

parameters. This indicates that the drugs adopt a specific conformation to form stable inclusion complex. However the CD also distorted to a great extent upon complexation.

In both drugs, the ΔE was attributed to bonded and non-bonded interactions, such as hydrogen bondings, electrostatic forces, and van der Waals interactions. The van der Waals interactions were the predominant driving force in the drug/CD complex, which is supported by the results reported in literature [24, 25]. The results in Table 3 point to that the non-bonded interactions played an important role in the stability of the drug/CD complex, which was also essential for the complex formation.

The enthalpy change (ΔH) for the inclusion complexation of EPIN/β-CD (−11.67 kcal.mol^{-1}) was more negative than

Table 3 Energetic features, thermodynamic parameters and HOMO-LUMO energy calculations for EPIN, NORE, α-CD, β-CD and its inclusion complexes by PM3 method

Properties	NORE	EPIN	α-CD	β-CD	NORE/α-CD	NORE/β-CD	EPIN/α-CD	EPIN/β-CD
E[a]	−113.94	−112.85	−1247.62	−1457.75	−1370.95	−1583.02	−1370.77	−1583.49
ΔE[a]					−9.39	−11.33	−10.30	−12.89
H[a]	11.74	30.07	−570.84	−667.55	−565.81	−666.04	−548.05	−649.15
ΔH[a]					−6.71	−10.23	−7.28	−11.67
G[a]	−20.82	−6.28	−676.37	−789.52	−685.01	−805.86	−668.16	−790.04
ΔG[a]					12.18	4.48	14.49	5.76
S[b]	0.109	0.121	0.353	0.409	0.399	0.468	0.402	0.472
ΔS[b]					−0.063	−0.05	−0.072	−0.058
E_{HOMO} (eV)	−9.11	−8.89	−10.37	−10.35	−8.79	−8.77	−8.76	−8.95
E_{LUMO} (eV)	0.01	0.27	1.26	1.23	0.22	0.24	0.26	0.07
$E_{HOMO-LUMO}$ (eV)	−9.12	−9.16	−11.63	−11.58	−9.01	−9.02	−9.02	−9.02
Dipole moment (D)	1.67	2.33	11.34	12.29	10.90	10.67	11.13	11.07

[a] –kcal.mol^{-1} ; [b] –kcal/mol-Kelvin

that of other inclusion complexes, which is certainly attributed to the more tightly van der Waals interactions between CD and guest [26]. Thus, we can conclude that the effect of the methyl groups upon the complexation is to strengthen the van der Waals interactions. The negative enthalpy changes together with the negative entropy changes suggest that all the inclusion processes are enthalpy-driven in nature. From the PM3 calculations, we also noticed that the dipole moment values of free drugs increase when the hydrophobic guest enters into the CD nano-cavity and the complex is formed. Further the variation of dipole moment in different complexes indicates a strong correlation of the polarity with the inclusion process.

Solid Inclusion Complex Studies

It has been extensively demonstrated that the co-precipitation method used for the preparation of drug-CD solid inclusion complexes can significantly affect the physicochemical as well as dissolution properties of the obtained solid systems [27, 28]. In this regard, an equimolar NORE/CD and EPIN/CD solid inclusion complexes were prepared and the encapsulated drugs carefully characterized by SEM, TEM, FT-IR, ^{1}H NMR, DSC and XRD analyses.

Microscopic Morphological Observations by SEM and TEM

In order to study the morphological changes, first we recorded the images of the powdered form of pure NORE, EPIN, α-CD and β-CD by SEM and then we also observed powdered form of the inclusion complexes (Fig. S1). These pictures clearly elucidated the difference between the pure drugs and their inclusion complexes. It is clear from the SEM images that (i) α-CD particles presents prismatic with well-developed faces whereas plated shape was observed for β-CD particles, (ii) drugs are present in different form from their inclusion complexes. The difference in the structure of pure drugs and the inclusion complexes support the presence of solid inclusion complex. Morphological changes of these structures can be taken as a proof for the formation of a new inclusion complex.

TEM photographs are usually employed to investigate the CD based self-aggregated nanostructures such as nanotubes, nanorods and vesicles in aqueous solution [29, 30]. Therefore, the morphology of freshly prepared drug-CD inclusion complexes was observed using TEM (Fig. S2). Significant differences in size and shape among the two encapsulated drugs with CDs were observed; that is, for the freshly synthesized NORE/CD complexes, approximately in the range of 47~110 nm nano-sized particles were observed. Interestingly, in the case of EPIN/CD complexes, a beautiful aggregation of the nanoparticles (flower-like structure) with halo space was observed (Figs. S2c and S2d). The insert Fig. S2d clearly illustrates that such kind of structure is actually assembled by several smaller nanoparticles. This picture provides important information about the above assumption for the formation of flower-like structures. This study might be of great important for the applications of nanoparticles in drug-delivery, smart materials and biosimulation.

FT-IR Spectral Studies

The FT-IR spectra of NORE, EPIN drugs and their corresponding solid inclusion complexes are presented in Figs. S3 and S4. CD showed prominent peaks at 3,300, 1,638, 1,035 and 564 cm^{-1} as related in the literature. In both CDs (Figs. S3 and S4), the bands in the wavenumber range 500–1,500 cm^{-1} not arises from a single type of molecular vibration. This is due to strong coupling of vibrations from the macrocyclic ring, caused by similar frequencies of neighboring bonds vibrations.

NORE showed a strong band at 3,389 cm^{-1} for NH stretching vibration (Fig. S3c). The band at 3,153 cm^{-1} was noticed for stretching vibration of phenolic –OH groups. The absorption peaks at 1,516, 1,442 and 1,606 cm^{-1} was corresponding to the C = C stretching in the aromatic ring and the NH_2 deformation vibration. The absorption bands corresponding to C-OH in-plane bending vibration and O-H out-of-plane deformation were observed at 1,358, 1,282 and 603 cm^{-1}. Further the band at 2,950 cm^{-1} was obtained for CH stretching of methylene group. The NORE/CD inclusion complexes did not show any new peaks, suggesting no chemical bonds were formed in the complex. However, the inclusion complex band altered with the peak in 3,389 cm^{-1} largely moved to 3,402 cm^{-1} in α-CD complex and 3,400 cm^{-1} in β-CD complex indicated that the amino group of NORE was entrapped into the CD nano-cavities. This is confirmed by the NH_2 deformation vibration at 1,606 cm^{-1} also shifted (1,643 cm^{-1} for α-CD complex and 1,647 cm^{-1} for β-CD complex). This is due to the aliphatic chain entrapped into the CD cavity. The C = C stretching vibration of aromatic ring (1,516 cm^{-1}) disappeared in the inclusion complex, and the intensity of band for CH_2 deformation (1,442 cm^{-1}) reduced and shifted to 1,410 cm^{-1} and 1,419 cm^{-1}. Further the CH stretching of methylene group also shifted in the inclusion complexes (Figs. S3d and S3e). These results indicated that due to the formation of inclusion complex, the vibration mode of NORE molecule was restricted and the aliphatic chain was inserted deeply into the CD cavity.

In EPIN (Fig. S4a), the NH stretching vibrations at 3,331 and 3,272 cm^{-1} was shifted to higher frequencies in the complex. The NH deformation vibrations appeared at 711 and 740 cm^{-1}, but both peaks shifted in the spectra of inclusion complexes to ~707 cm^{-1}. The phenolic OH out-of-plane deformation vibrations for the EPIN drugs appeared at ~650 and 632 cm^{-1} are shifted to the shorter frequencies. The OH stretching frequency at 3,020 and 3,161 cm^{-1} respectively, was also shifted longer wave number in the inclusion

complex. The bands corresponding to the overtones and combinations of aromatic ring appeared at 1,842 and 1,738 cm^{-1} but these two bands are disappeared in the complex spectrum. The four bands in the region 1,625–1,430 cm^{-1} for aromatic C = C stretching was also moved in the complex to longer frequencies. Also, the aromatic ring deformation at 534 cm^{-1} was moved to ~510 cm^{-1} in the inclusion complex. However, the absorption intensity of the inclusion complex was also significantly varied from free drug. The above results confirmed that the drug molecules were included into the CD nano-cavity.

DSC Studies

Differential scanning calorimetry (DSC) represents an effective and inexpensive analytical tool for an accurate physicochemical characterization of encapsulation (drug-CD) systems in the solid state and is widely used for a rapid preliminary qualitative investigation of the thermal behavior of the single components, their physical mixtures and the inclusion compound prepared according to a standard procedure such as coprecipitation.

DSC analysis reveals some evidence for the formation of inclusion complex between EPIN, NORE and α-CD/β-CD, which shows the difference between the isolated materials and the inclusion complexes. The DSC of pure drugs and the inclusion complexes of EPIN/CD and NORE/CD are presented in Fig. S5. It could be seen in Fig. S5a and S5d that the above drug molecules exhibited sharp endothermic peaks at 217.5ºC and 211.5ºC, respectively. This phenomenon was caused by the melting point of drugs. The DSC profile of α-CD showed three endothermic peaks at ~79, 109, 137 °C and a broad endothermic peak at ~128 °C was observed for β-CD. These endothermic effects are mostly associated to crystal water losses from CD cavities. In contrast, the DSC curves of solid inclusion complexes differed from those of pure components. However, in the DSC curves of the solid complexes, the endothermic peaks corresponding to the free drug disappeared, coinciding with the shift of the endothermic peaks corresponding to the free CD's dehydration process to lower temperatures. These observations indicated that the formation of drug-CD inclusion complexes retarded the melting of EPIN and NORE during heating, suggesting the thermal stability of drug molecules was improved when it was encapsulated by host CD molecules.

^{1}H NMR Spectral Studies

Proton nuclear magnetic resonance (^{1}H NMR) spectroscopy has proved to be a powerful tool in the study of inclusion complexes [14, 19]. ^{1}H NMR spectroscopy provides an effective means of assessing the dynamic interaction site of CD with that of the guest molecules. The basis of information gained from NMR spectroscopy is located in this shifts, loss of resolution and broadening of signals observed for the host and guest protons [14, 19]. In this study, to analyze the interaction behavior of the drugs with hydrophobic CD nano-cavities, ^{1}H NMR spectra of the guest in the absence and presence of equimolar CD in DMSO-d_6 were measured (Fig. S6). The resonance assignments of the protons of CD are well established and consist of six types of protons. The chemical shift of CD protons reported by different authors are very close to those reported in this work. The H-3′ and H-5′ protons are located in the interior of the CD cavity, and it is, therefore likely that the interaction of the guest with the CD inside the cavity will affect the chemical shifts of those protons. A minor shift is observed for the resonance of H-1′, H-2′ and H-4′ located on the exterior of CD.

The assignments of the drug EPIN are shown as inset in Fig. S6a. EPIN showed evidence of inclusion by α-CD/β-CD with substantial changes in chemical shift caused by the presence of CD. Here the formation of inclusion complex could be proved from the comparison of the chemical shifts of drugs before and after interaction with CD, which was defined as $\Delta\delta = \delta_{complex} - \delta_{free}$. The chemical shifts values for EPIN (δ, in ppm) and the changes in chemical shift (Δδ) observed on complexation with α-CD/β-CD (in parentheses) are as follows: H_a = 6.709 (0.014/0.016), H_b = 6.632 (0.002/0.003), H_c = 6.536 (−0.009/−0.011), H_d=4.443 (0.008/0.012) and H_g = 2.290 (0.012/0.016). In the CD complex, the resonance signals of aliphatic as well as aromatic protons significantly decreased and CD proton signals were shifted and merged, which indicates that the guests were entrapped inside the CD cavity and that their flexibility was affected by non-covalent interactions [31, 32]. The guest within the CD cavity obviously experienced a shielding effect. The drug with the additional side-chain methyl group at H_g protons of EPIN had the largest Δδ value in the molecule. While the Δδ values for the aromatic protons H_b are small or insignificant on complexation with CD. Although it could not be measured the Δδ value for H_e and H_f, because the shifted signal was obscured by CD or solvent peaks. It can also be observed from the results that the signals were shifted to a lesser extent with α-CD than when β-CD was added and the direction of the shift almost similar in both cases. However, the broadening of the proton signals of guest in the presence of CD suggested that the motions of these protons were restricted [33]. Significant shifts were observed in the alkyl chain protons and aromatic region of EPIN spectra on complexation with both CDs are indicate that this part of the drug molecule entrapped in the hydrophobic nano-cavities of the macromolecules.

XRD Analysis

Powder X-ray diffractometry (XRD) is a useful for the detection of CD encapsulation and it has been used to assess the degree of crystallinity of the given sample. When a true complex is formed, the overall numbers of crystalline structure are

reduced and more number of amorphous structures is increased. Hence, the solid complexes exhibit less number as well as less intensity peaks. This shows that overall crystallinity of complex is decreased and due to amorphous halo nature, the solubility is increased. Hence, the XRD patterns of EPIN and NORE as well as their inclusion complexes with α-CD/β-CD in powder form were collected at diffraction angle (2θ) from 5º to 50º and are illustrated in Fig. S7. As indicated in Fig. S7c the EPIN drug was in a well crystalline form. The XRD pattern of α-CD showed the characteristic peaks at 2θ values of 9.46°, 11.82°, 14.19°, 17.93°, 21.57° and 27.12°. However, the diffractogram of β-CD crystals exhibited the important peaks at 2θ values of 8.95°, 10.56°, 12.46°, 18.75°, 22.57°, 27.03°, 31.86° and 34.59°. Most of the characteristic peaks of drugs were present in the diffraction patterns of physical mixtures of the drug with CDs without loss intensity. In contrast, the XRD of the NORE/α-CD, NORE/β-CD, EPIN/α-CD and EPIN/β-CD complexes are amorphous and show halo patterns, which are quite different from the superimposition (physical mixture) of crystalline drugs in α-CD and β-CD, indicating the formation of the inclusion complex between α-CD or β-CD and EPIN or NORE. In addition, most of the crystalline diffraction peaks of α-CD and β-CD disappeared after complexation with drugs, indicating that the complexation of drugs oriented in the CD cavities to some extent.

Conclusions

The following conclusions can be drawn from the above studies: In aqueous solutions, both CDs have been found to be formed inclusion complexes with NORE and EPIN. Addition of drugs to aqueous solutions of CD has resulted in the observation of the excimer fluorescence i.e., 1:2 CD- $drug_2$ inclusion complex. Semiempirical calculations confirm the hydrogen bonds were the driving force for the inclusion process and also responsible for the complexes stability. The negative enthalpy change (ΔH) suggested that all these inclusion processes were exothermic. The statistical thermodynamic calculations suggested that these inclusion complex processes are enthalpically favourable in nature. Both experimental and theoretical methods proved that drugs were partially included in the hydrophobic CD nanocavity with the alkyl chain located near the primary rim and the phenyl ring near secondary rim. Investigations of SEM, TEM, FT-IR, ^{1}H NMR, DSC and XRD results showed important modifications in the physicochemical properties of the drug molecules through the formation of inclusion complexes.

Acknowledgments This work is supported by the Council of Scientific and Industrial Research [No. 01(2549)/12/EMR-II] and University Grants Commission [F.No. 41-351/2012 (SR)] New Delhi, India. The authors thank Dr. P. Ramamurthy, Director, National centre for ultrafast processes, Madras University for help in the fluorescence lifetime measurements for this work.

References

1. Xue QH (1978) Physiological and pathological chemistry of nervous system. Science Press, Beijing Science Press, Beijing
2. Sun S, Weil MH, Tang W, Kamohara T, Klouche K (2001) Alpha-methylnorepinephrine, a selective alpha$_2$-adrenergic agonist for cardiac resuscitation. J Am Coll Cardiol 37:951
3. Efrati O, Barak A, Ben-Abraham R, Modan-Moses D, Berkovitch, Manisterski Y, Lotan D, Barzilay Z, Paret G (2003) Should vasopressin replace adrenaline for endotracheal drug administration? Crit Care Med 31:572
4. Manisterski Y, Vaknin Z, Ben-Abraham R, Efrati O, Lotan D, Berkovitch M, Barak MA, Barzilay Z, Paret G (2002) Endotracheal epinephrine: a call for larger doses. Anesth Analg 95:1037
5. Martin Del Valle EM (2004) Cyclodextrins and their uses: a review. Process Biochem 39:1033
6. Carrier RL, Miller LA, Ahmed I (2007) The utility of cyclodextrins for enhancing oral bioavailability. J Control Release 123:78
7. Loftsson T, Brewster ME (1996) Pharmaceutical applications of cyclodextrins. 1. Drug solubilization and stabilization. J Pharm Sci 85:1017
8. Szejtli J (1998) Introduction and general overview of cyclodextrin chemistry. Chem Rev 98:1743
9. Fromming KH, Szejtli J (1994) Cyclodextrins in pharmacy. Kluwer Academic Publishers, Dordrecht, p 413
10. Yan C, Li X, Xiu Z, Hao C (2006) A quantum-mechanical study on the complexation of β-cyclodextrin with quercetin. J Mol Struct (THEOCHEM) 764:95
11. Seridi L, Boufelfel A (2011) Molecular modeling study of Lamotrigine/β-cyclodextrin inclusion complex. J Mol Liq 158:151
12. Premakumari J, Allan Gnana Roy G, Antony Muthu Prabhu A, Venkatesh G, Subramanian VK, Rajendiran N (2011) Spectral characteristics of sulphadiazine, sulphisomidine: effect of solvents, pH and β-cyclodextrin. Phys Chem Liq 49:108
13. Antony Muthu Prabhu A, Venkatesh G, Rajendiran N (2010) Spectral characteristics of sulfa drugs: effect of solvents, pH and β-cyclodextrin. J Solut Chem 39:1061
14. Antony Muthu Prabhu A, Subramanian VK, Rajendiran N (2012) Excimer formation in inclusion complexes of β-cyclodextrin with salbutamol, sotalol and atenolol: spectral and molecular modeling studies. Spectrochim Acta A 96:95
15. Sankaranarayanan RK, Siva S, Venkatesh G, Antony Muthu Prabhu A, Rajendiran N (2011) Dual fluorescence of dothiepin, doxepin drugs—effect of solvents and β-cyclodextrin. J Mol Liq 161:107
16. Antony Muthu Prabhu A, Venkatesh G, Rajendiran N (2010) Unusual spectral shifts of imipramine and carbamazepine drugs. J Fluoresc 20:1199
17. Venkatesh G, Thulasidhasan J, Rajendiran N (2014) A spectroscopic and molecular modeling studies of the inclusion complexes of orciprenaline and terbutaline drugs with native and modified cyclodextrins. J Incl Phenom Macrocycl Chem 78:225–237
18. Antony Muthu Prabhu A, Rajendiran N (2012) Encapsulation of Labetalol, Pseudoephedrine in β-cyclodextrin Cavity: Spectral and Molecular Modeling Studies. J Fluoresc 22:1461
19. Sivasankar T, Antony Muthu Prabhu A, Karthick M, Rajendiran N (2012) Encapsulation of vanillylamine by native and modified cyclodextrins: spectral and computational studies. J Mol Struct 1028:57
20. Paul BK, Samanta A, Guchhait N (2010) Modulation of excited-state intramolecular proton transfer reaction of 1-hydroxy-2-naphthaldehyde in different supramolecular assemblies. Langmuir 26:3214
21. Mallick A, Haldar B, Maiti S, Bera SC, Chattopadhyay N (2005) Photophysical study of 3-acetyl-4-oxo-6,7-dihydro-12H-indolo[2,3-a]quinolizine in biomimetic reverse micellar nanocavities: a spectroscopic approach. J Phys Chem B 109:14675

22. Das P, Chakrabarty A, Haldar B, Mallick A, Chattopadhyay N (2007) Effect of cyclodextrin nanocavity confinement on the photophysics of a beta-carboline analogue: a spectroscopic study. J Phys Chem B 111:7401
23. Singh RB, Mahanta S, Guchhait N (2008) Study of interaction of proton transfer probe 1-hydroxy-2-naphthaldehyde with serum albumins: a spectroscopic study. J Photochem Photobiol B 91:1
24. Yan CL, Xiu ZL, Li XH, Hao C (2007) Molecular modeling study of beta-cyclodextrin complexes with (+)-catechin and (-)-epicatechin. J Mol Graph Model 26:420
25. Chaudhuri S, Chakraborty S, Sengupta PK (2010) Encapsulation of serotonin in β-cyclodextrin nano-cavities: fluorescence spectroscopic and molecular modeling studies. J Mol Struct 975:160
26. Rekharsky MV, Inoue Y (1998) Complexation thermodynamics of cyclodextrins. Chem Rev 98:1875
27. Chen W, Yang LJ, Ma SX, Yang XD, Fan BM (2011) Crassicauline A/β-cyclodextrin host–guest system: preparation, characterization, inclusion mode, solubilization and stability. Carbohydr Polym 84:1321
28. Yang LJ, Chen W, Ma SX, Gao YT, Huang R, Yan SJ (2011) Host–guest system of taxifolin and native cyclodextrin or its derivative: preparation, characterization, inclusion mode, and solubilization. Carbohydr Polym 85:629
29. Jing B, Chen X, Wang X, Yang C, Xie Y, Qiu H (2007) Self-assembly vesicles made from a cyclodextrin supramolecular complex. J Chem Eur 13:9137
30. Li G, McGown LB (1994) Molecular nanotube aggregates of β-cyclodextrins and γ-cyclodextrins linked by diphenylhexatrienes. Science 264:249
31. Eliadou K, Yannakopoulou K, Rontoyianni A, Mavridis IM (1999) NMR Detection of Simultaneous Formation of [2]- and [3]Pseudorotaxanes in Aqueous Solution between α-Cyclodextrin and Linear Aliphatic α,ω-Aminoacids, an α,ω-Diamine and an α,ω-Diacid of Similar Length, and Comparison with The Solid State Structures. J Org Chem 64:6217
32. Steed JW, Foster JA (2010) Exploiting cavities in supramolecular gels. Angew Chem Int Ed 49:6718
33. Chao J, Li JS, Meng DP, Huang S (2003) Preparation and study on the solid inclusion complex of sparfloxacin with HP-beta-cyclodextrin. Spectrochim Acta Part A Mol Biomol Spectrosc 59:705